



RAPID ESTIMATES OF EARTHQUAKE-INDUCED MASS MOVEMENTS AND LIQUEFACTION LIKELIHOODS IN SWITZERLAND VIA SHAKEMAP

C. Cauzzi⁽¹⁾, D. Fäh⁽²⁾, D. Wald⁽³⁾, J. Clinton⁽⁴⁾ & S. Wiemer⁽⁵⁾

⁽¹⁾ *Researcher & Lecturer, Swiss Seismological Service (SED) at ETH Zürich, carlo.cauzzi@sed.ethz.ch*

⁽²⁾ *Professor, Swiss Seismological Service (SED) at ETH Zürich, donat.fae@sed.ethz.ch*

⁽³⁾ *Research Geophysicist & Professor, United States Geological Survey (USGS) at Golden, Colorado, wald@usgs.gov*

⁽⁴⁾ *Director of Seismic Networks, Swiss Seismological Service (SED) at ETH Zürich, jclinton@sed.ethz.ch*

⁽⁵⁾ *Professor & Director of the SED, Swiss Seismological Service (SED) at ETH Zürich, stefan.wiemer@sed.ethz.ch*

Abstract

In Switzerland, nearly all historical $M_w \sim > 6$ earthquakes are associated to damaging rockslides, resulting in some cases into destruction of settlements and loss of lives. Liquefaction is known to have occurred historically due to the 1855 M_w 6.2 earthquake of Visp, where the valley floor is presently highly built and industrialised. We describe in this contribution the customisation to Swiss conditions of globally calibrated empirical approaches for the near-real-time estimation of earthquake-induced landslide and liquefaction likelihoods. We parameterise the probability of occurrence of these secondary hazards through a set of georeferenced susceptibility proxies (*e.g.*, geomorphology, surface geology, ground types, soil wetness) and intensity measures (*e.g.*, intensity-derived peak ground acceleration, *PGA*). The coefficients of the predictive models are calibrated against the shaking constraints from past events and optimised for near-real-time estimates based on USGS-style ShakeMaps used at SED since 2007. Emphasis is on the use of high-resolution topographic datasets along with geological and geotechnical information available in the Swiss context. This study facilitates future investigations on the rapid assessment of the likelihood of earthquake-induced lake tsunamis triggered by underwater landslides and has a high practical relevance to Swiss ShakeMap end-users and stakeholders managing lifeline systems.

Keywords: ShakeMap, landslides, liquefaction

1. Introduction and motivation

ShakeMap is a well-known scientific and technical framework that provides near real-time seismic shaking scenarios based on recorded and predicted ground motions, response spectra and macroseismic intensity levels, including amplification due to local site effects.

The last few years have witnessed a major revision of the rapid earthquake scenarios distributed by the Swiss Seismological Service (SED) based on the United States Geological Survey (USGS) ShakeMap software [1, 2, 3] first introduced in Switzerland by [4]. The most important changes already tested and implemented are: i) a new set of predictive equations for ground shaking parameters, spectral acceleration levels [5] and macroseismic intensity [6]; ii) a comprehensive revision of the strategy used to account for local site amplification at regional [7] and seismic station level [8]; iii) the implementation of the previous points in the latest ShakeMap3.5 framework [1, 2, 3]; iv) the development of the software module "scwfpparam" enabling ShakeMap computation based on the earthquake monitoring system SeisComp3 [9] used at the SED. These scientific and technical efforts - documented in [10, 11, 12] - ensure consistency of the "Next Generation Swiss ShakeMap" (Fig. 1, see also <http://shakemapa.ethz.ch>) with current engineering seismology science in Switzerland, mainly driven by the research activities of the SED. While the present update adequately fulfils the mandate of SED to deliver to researchers and the general public rapid and fairly detailed shaking scenarios for relevant / felt events, improvements are possible and solicited as to the prediction of secondary hazards and the integrated use of the data collected through online questionnaires ("Did You Feel It?", DYFI) and processed both automatically and manually at the SED. Natural candidates for secondary hazards to focus on within the ShakeMap framework are earthquake-induced mass movements and soil liquefaction.

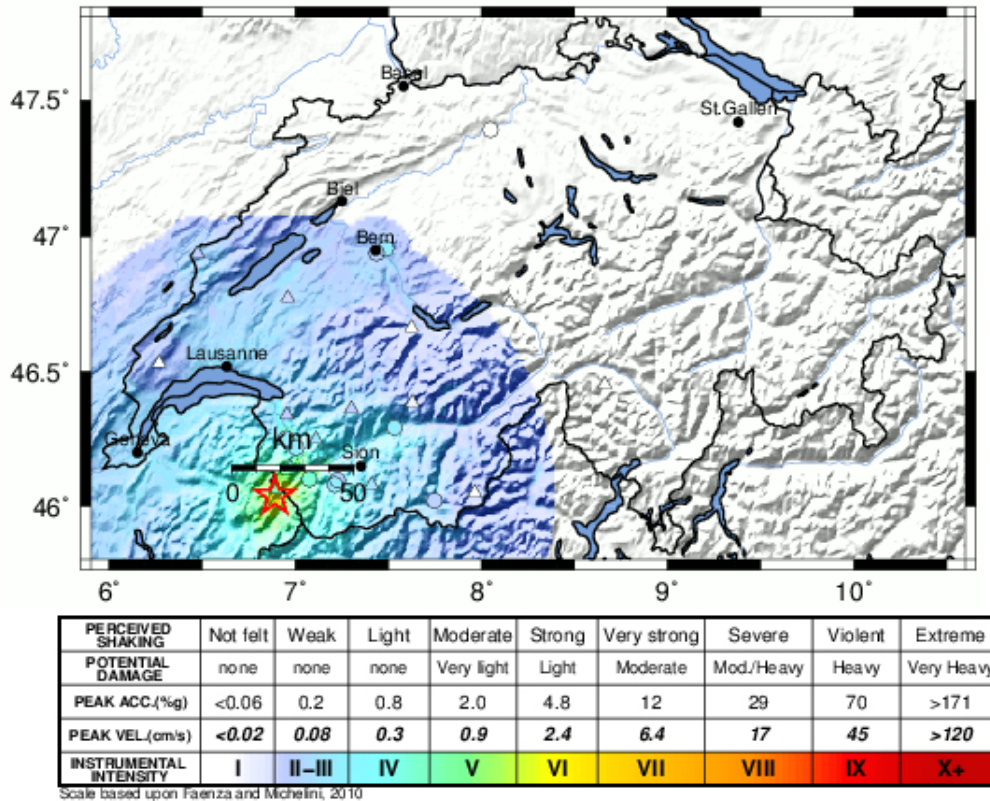


Fig. 1 – SED ShakeMap for the 2005 M_w 4.4 Vallorcine (Switzerland / France border) event computed as described in the text. The shaking intensity accounts for all available on-scale broadband and strong-motion recordings (triangles) of the Swiss national seismic networks along with high-quality felt reports (DYFI, shown as circles). The star indicates the location of the epicentre.

Mass movements induced by earthquakes are a major threat in mountain regions because of their severe impacts on urban settlements and lifeline systems [13]. Typical failures include landslides, rockfalls and avalanches. Approximately 5% of all earthquake-related fatalities worldwide are caused by landslides triggered by earthquake shaking [14]. In Switzerland, nearly all historical $M_w \sim 6$ or larger earthquakes [7] are associated to damaging rockslides and landslides, resulting in some cases into destruction of settlements and loss of lives [15, 16, 17]. Earthquake-triggered ocean and lake tsunamis generated by underwater landslides and rockfalls are also well documented. Notable in the international literature is the case of the 1929 Grand Banks earthquake [18]. In Switzerland, the earthquakes of Aigle 1581 and Unterwalden 1601 are associated with lake tsunamis most likely due to underwater mass movements [19, 20]. Even when the urban environment is not directly hit by the aforementioned phenomena, a high risk of deadly impacts still exists, as dramatically experienced by the many climbers killed by avalanches and rockfalls triggered by the recent Nepal (April 2015) and the Sabah, Malaysia (June 2015) earthquake.

The landslide susceptibility in case of earthquake shaking is studied in the international literature either by means of a) mechanical models (*e.g.*, [21]) based on the classical approach of [22] or b) statistical models (*e.g.*, [23]) where the probability of landslide occurrence is parameterised through a set of georeferenced landslide susceptibility proxies (*e.g.*, geomorphology, surface geology, ground types) and ground shaking parameters. While both approaches have physical bases, (a) seems scientifically more elegant as it relies on basic principles of soil mechanics while (b) - fairly comparable to the methods used in empirical prediction of ground motions based on recorded datasets - aims at optimising the use of easily accessible explanatory variables combined through simple functional forms, with coefficients calibrated against the observations of past events. Approach (a) is the natural candidate for assessing long-term landslide potential in relatively small and well known study

areas, while (b) is optimised for near real-time estimates at regional level, *i.e.*, the traditional domain of USGS-style ShakeMaps.

The surface expression of soil liquefaction is a critical secondary effect in the perspective of rapid response, loss estimation, and emergency planning due to its often large impact on lifeline systems, industrial and residential settlements. Recent moderate events associated with extensive liquefaction observations occurred in Christchurch, New Zealand, in 2010 [24] and Mirandola, Italy, in 2012 [25]. These earthquakes have the typical size of damaging Swiss alpine events [7]. In Switzerland, liquefaction is known to have historically occurred *e.g.* after the 1855 M_W 6.2 earthquake of Visp, where the valley floor is presently highly built and industrialised [26]. The classical approaches of soil dynamics to evaluating liquefaction potential require knowing the density, cohesion, grain size distribution, plasticity index and water saturation of the soil column and the dynamic load imposed by the earthquake in terms of both shaking amplitude and duration (*e.g.*, [27, 28]). Soil characterisation and water table depth would require site-specific investigations including geotechnical logs and penetration data but first order evaluations of the liquefaction likelihood for a given area can be attempted if simple proxies for these soil characteristics are identified.

With this motivation, we selectively present in this paper the use of globally calibrated empirical approaches ([23, 29] and subsequent updates) to estimating the landslide and liquefaction likelihood for moderate-to-strong events in Switzerland. With these approaches, the probability of occurrence of the aforementioned secondary hazards is parameterised through a set of georeferenced susceptibility proxies (*e.g.*, geomorphology, surface geology, ground types, soil wetness) and ground shaking parameters (*e.g.*, peak ground acceleration, PGA). These approaches rely on using easily accessible explanatory variables combined through simple functional forms with coefficients calibrated against the observations of past events and are optimised for near real-time estimates based on USGS-style ShakeMaps.

Our strategy to customising the global approaches to Swiss conditions relies on the comparison between the estimates provided by the current USGS implementation of the global models [23, 29] with the historical observations of relevant events ($M_W \sim 6$; $I_{EMS-98} \geq VII$) in the Swiss earthquake catalogue ECOS-09 [7]. We derived corrective factors and actions for optimal implementation within the Swiss context. The earthquake catalogue of Switzerland and the compilation of earthquake-induced secondary effects by [15, 16, 17] provide a unique dataset to test the performance of the USGS global models in the Swiss Alps. ShakeMaps for these events (identified by the use of the keyword ECOS in the EventID and name) are available at <http://shakemap.ethz.ch/archive/scenario.html>. The ShakeMap intensity estimates used in this study include ECOS-09 macroseismic observations (intensity data points, IDPs – shown as circles in the online maps and in this manuscript) in the same way web-collected DYFI data are treated in ShakeMap3.5. Using historical scenarios implies deriving ground shaking parameters from macroseismic intensity fields based on the ground-motion to intensity conversion equations (GMICEs) of [6], suitable for the Swiss context [12]. Key to the customisation to Switzerland is the use of high-resolution (90 m and 30 m) geographic datasets along with geological and geotechnical information (*e.g.*, geological and geotechnical units characterisation, water table depth, mapped instabilities) typically not available at the global level and therefore not considered by [23, 29].

2. Mass movements

We started from the 2015 USGS implementation of the landslide likelihood model of [23] for rapid assessment of earthquake-triggered landslides worldwide. The predictive models uses ShakeMap peak accelerations, PGA [%g], as intensity measure, while the susceptibility to sliding is represented by the topographic slope S [$100 \cdot deg.$] and material cohesion c [MPa]. Previous versions of the model used material friction angle ϕ [$deg.$] rather than cohesion to represent the shear strength of geo-materials. The model coefficients were determined through logistic regressions, known to be appropriate for processes involving only a binary outcome. The landslide probability P is given by Eq. (1):

$$P = 1/(1+\exp(-X)) \quad (1)$$

where

$$X = const + f(PGA) + f(S) + f(PGA \cdot S) + f(c). \quad (2)$$

Consistent with the global ShakeMap approach, USGS *PGA* maps for global events are computed within ~ 10-30 minutes of the earthquake origin time based on NEIC (National Earthquake Information Center) location, magnitude and a ground-motion prediction model suitable for the region of interest (<http://earthquake.usgs.gov/earthquakes/shakemap/>). ShakeMaps are updated once earthquake recordings and finite-fault models become available, and automatically include raw (not revised by humans) DYFI intensity estimates. Topographic slope and material strength parameters at global scale are those computed by [30] and [31], who modified the [32] global classification and assigned friction angles and cohesion based on published values (*e.g.*, [33, 34]) for geological units. The landslide likelihood estimates are dominated by the *PGA* term, the slope term and the combined *PGA* and slope term. The contribution of the cohesion term to the likelihood estimates is negligible. Different from [23] who used the compound topographic index *CTI* [35] as predictor, the currently preferred model does not include any information about soil wetness. Earthquake triggered landslide likelihood is therefore dominated by *PGA* and topographic slope. The model is implemented as a Python package (Hearne M, pers. comm.) and not included in the ShakeMap distribution yet. The landslide likelihood estimates based on global ShakeMap are not made available to the public yet are sent to the USAID Office of Foreign Disaster Assistance (OFDA) for test evaluation of the product.

Notable amongst the earthquakes documented in the ECOS-09 catalogue is the 1946 M_w 5.8 Sierre event (Fig. 2) for which observations of secondary effects triggered by the mainshock and the strongest aftershock (M_w 5.5) are abundant [15]. The Sierre 1946 event is showed here as the test case to assess the performance of the global model and to propose corrective factors / modifications for use in Switzerland. Several tests were carried out using topographic slope data derived from Digital Elevation Models (DEM) with different spatial resolution, namely the global grid used by USGS, a regional 90m-resolution grid and the Swiss national 30m grid. Good results were obtained using a 30m-resolution DEM coupled with upper bound *PGA* estimates - *i.e.*, obtained from [6] as $PGA = PGA(I - \sigma)$, where *I* is the macroseismic intensity and σ is the standard deviation of the GMICE - and modifying the constant term of the USGS model based on residual analyses of the predicted landslide likelihood values as a function of the main explanatory variables. The spatial distribution of the historical observations clearly suggested that landslides and rockslides occurred at grid points where (*i*) the cross-term $PGA[\%g] \times slope [deg \times 100] > 104$. The predictive model was therefore modified to output values between 1 and 2 if condition (*i*) was matched. This means $P(landslide) > 0.75$ at these locations. We also decided to neglect the $f(c)$ term that had no significant impact on the overall predictions. The results are depicted in Fig. 3 (bottom left panel) where the computed landslide probabilities are shown along with the 30m-resolution background topography and the mainshock and aftershock triggered landslides (circles), rockfalls (diamonds) and avalanches (triangles) documented in [15]. The modified model also performed well for the Aigle 1584 (M_w 5.9) and the Visp-Stalden 1855 (M_w 6.2) historical scenarios used for validation, not shown here for brevity. With a few exceptions, the modified landslide model can satisfactorily represent the geographic distribution of the observations. The model seems to work better for rockfalls (where slope and ground shaking are the dominating factors) than for landslides (where the water content can play a significant role), and can capture the occurrence of the few (due to dry winter conditions) reported snow avalanches.

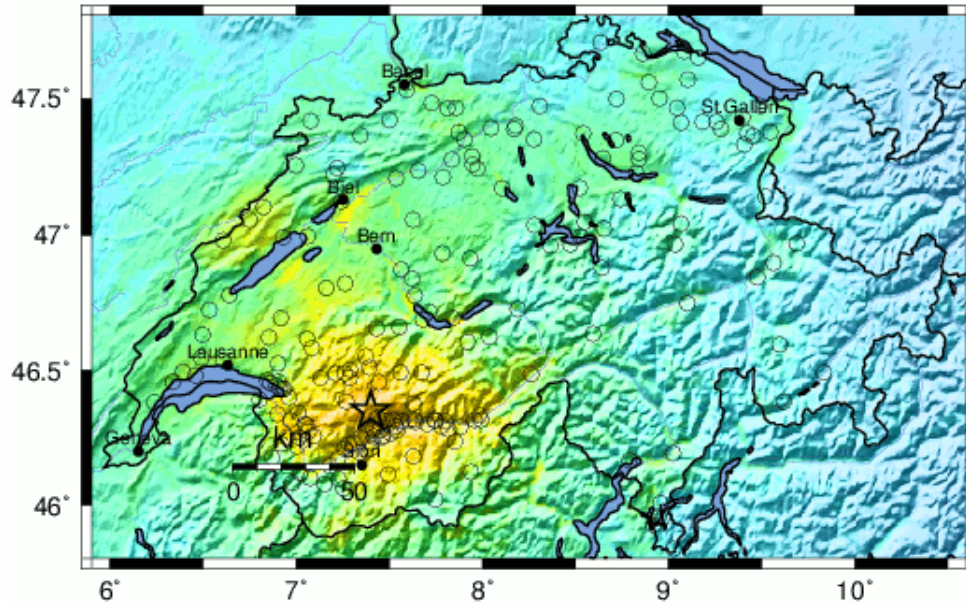


Fig. 2 – EMS-98 ShakeMap historical scenario of the 1946 M_w 5.8 Sierre (Valais, SW Switzerland) event, including macroseismic intensity data points from ECOS-09 shown as circles. The intensity colorscale is the same as Fig. 1.

This is our reason to refer to the model as a general “mass movement” likelihood model, even if originally developed for landslides. This is consistent with the fact that the ultimate cause of the failure is in all cases the exceedance of the shear strength of the geo-materials due to the additional loads imposed by the earthquake shaking often in combination with adverse meteorological conditions. The model has a notable ability to predict the spatial distribution of gravitational mass movement associated to aftershocks: the white diamond close to the epicenter in Fig. 3 (bottom panels) is the major (4-5 million cubic meters) Rawylhorn rockfall [15, 36]. There are large areas in Fig. 3, N and SW of the epicenter, where mass movements were not observed. It is not clear that these areas constitute “false positives”. According to [15] and [17], the secondary effects are well described in contemporary newspaper articles. However, a contemporary damage assessment carried out on behalf of the Canton Valais has survived in fragments only implying only partial completeness of the historical dataset. It is possible that the dip of the rock layers played a significant role in the distribution of the observed mass movements in the area. An attempt at mitigating possible “false-positives” and better constrain the mass movement predictions was carried out by [37], who explored the options to additionally / alternatively use: (a) frequency-dependent intensity measures (*e.g.*, PGA , PGV and response spectral ordinates); (b) different geomorphological proxies; and (c) maps of geological hazards (instabilities) recently compiled and delivered by the Swiss Cantons (Fig. 3, top panels). Given the limited number of observations available in the Swiss context, it was not possible to derive any strong conclusions based on (a) and (b) – although it was clear that mid-to-long-period intensity measures could better than PGA capture the geographic extent of known mass movements – while (c) appeared to be a promising approach. An example of the applications of strategy (c) is shown in Fig. 3 (bottom right panel) where the mass movement likelihood is convolved with information on the actual rockfall hazard as mapped by cantonal authorities. As apparent from Fig. 3, the cantonal information help to better constrain the predictions and capture the distribution of reported rockfalls. A similar exercise can be carried out for landslides and avalanches, not shown here for brevity.

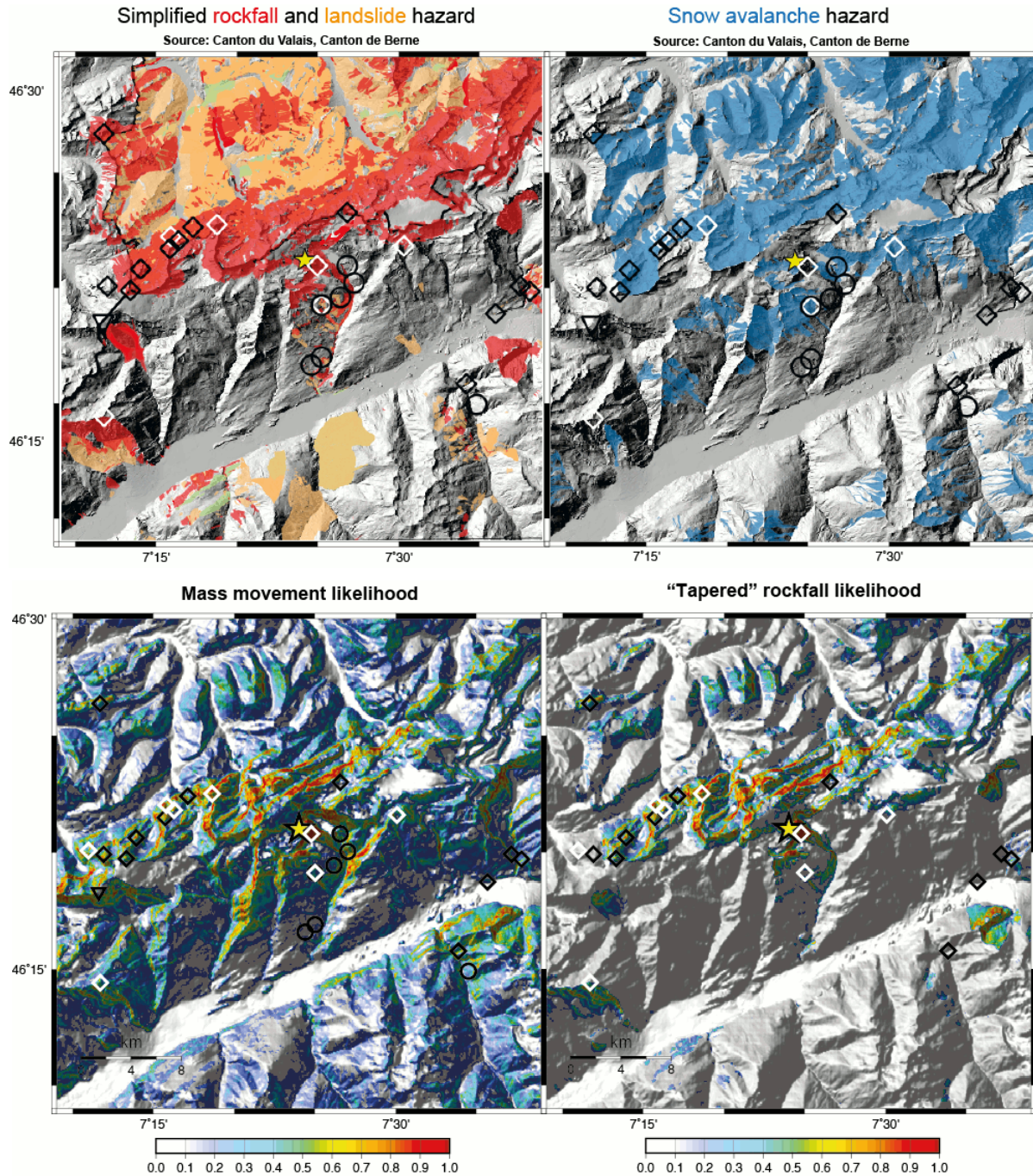


Fig. 3 – Top: simplified maps of geological hazards. Bottom left: mass movement likelihood for of the 1946 M_w 5.8 Siere (Valais, SW Switzerland) event computed as explained in the text. The yellow star shows the earthquake epicentre. Other symbols are rockfalls (diamonds), landslides (circles) and avalanches (triangles) triggered by the mainshock (black symbols) and the largest aftershock (white symbols). The rockfall and landslide patterns to the East and in the close proximity of the epicenter are particularly well captured. Bottom right: rockfall likelihood scenarios obtained using additional cantonal information on the actual rockfall hazard.

3. Liquefaction

Prototype near-real-time liquefaction likelihood estimates in development by USGS based on global ShakeMaps are computed using the global model of [29]. Similar to the landslide model discussed in the previous Section, the liquefaction probability is given by Eq. (1), where:

$$X = \text{const} + f(\text{PGA}, M_w) + f(\text{CTI}) + f(V_{S,30}). \quad (3)$$

PGA is ShakeMap peak ground acceleration in *g*, *CTI* is the compound topographic index [35] and $V_{S,30}$ is the travel time averaged shear-wave velocity in the uppermost 30 m of the soil column. The model uses a magnitude-weighting factor for *PGA* to represent the effects of the duration of significant shaking on the likelihood estimates. While all terms significantly contribute to the likelihood estimates, the likelihood estimates are dominated by the global *CTI* values and the topographic slope *S*. Although the topographic slope is not explicitly used in Eq. (3), the liquefaction likelihood is set to 0 if $S > 5 \text{ deg}$.

The adaptation of the global USGS liquefaction model to Switzerland was mainly based on historical earthquake scenarios of the 1855 Visp-Stalden (M_w 6.2, Fig. 4) and 1356 Basel (M_w 6.6) events. For the Visp-Stalden case, plausible historical sources mention ground deformation in the northern part of Visp that can be associated to lateral spreading of liquefied soils and widespread settlement due to ground liquefaction [17, 26]. The water table depth in the urban area is presently ~ 1.5 m. The global USGS model required $V_{S,30}$ as input. A $V_{S,30}$ map for Switzerland was computed by [38] based on macroseismic intensity increments ΔI [7]. We updated the $V_{S,30}$ estimates of [38] using a reference $V_{S,30} = 1100 \text{ ms}^{-1}$ [39] and the GMICE of [6] for *PGV*. We recomputed *CTI* values on a 90m-resolution DEM of the greater Swiss region to overcome the difficulties posed by using a low-resolution global (HYDRO1k dataset) *CTI* grid that can fail to accurately represent flow accumulation and catchment areas in relatively narrow Alpine valleys. Consistent with [40], we observed that increasing the resolution of the digital elevation model resulted into significantly higher levels of the *CTI* and therefore we scaled the results to match the *CTI* range used for calibrating [29].

The results shown in Fig. 4 (bottom panel) are consistent with the historical observations and the numerical simulations of [26]. However, application of the model to the Basel 1356 earthquake scenario showed that the use of *PGA* (which approaches 1g in this case), $V_{S,30}$ and *CTI* as predictors might lead to overestimating the liquefaction potential in the Basel region. Although water table depth varies between 0 and 4 m in the area, liquefaction is considered as of minor importance in Basel because, due to the geological conditions of the area, water-saturated, cohesionless, granular sediments at depths less than 10 are found only in a few places [41]. This motivated a correction of the liquefaction scenarios based on information on the surface geology and water table depth, *e.g.* convolving the output of the global liquefaction model with maps of cohesionless saturated granular materials. Such mapping is feasible for Switzerland either (a) by merging information from the national geological map and hydrological atlas; or (b) using units 5 and 6 of the “geotechnical map of Switzerland” (representing sands and gravels with different levels of fine content, correspondingly) with weighting factors of 0.5 and 1.0, respectively; or (c) using the national map of ground types (*i.e.*, similar to (b) but with different input).

For the Visp-Stalden 1855 scenario, the three models developed by [29] based on the Christchurch 2011 (M_w 6.2) dataset were also tested. Results consistent with the historical observations were obtained applying model no. 3 of [29], that uses *PGA*, $V_{S,30}$ and *dr* (the distance to rivers, that replaces *CTI* as a proxy for soil wetness) as predictors. For implementation in Swiss ShakeMap, it is recommended to implement both the global and the Christchurch no.3 model of [29] and estimate the likelihood of liquefaction as the average output of the two models, as shown in Fig. 4. Note that the two approaches represent viable alternatives as they employ different proxies for soil wetness. In areas where liquefaction of lake sediments may occur, it is also possible to implement prediction models based on *ND*, that is the normalised coast distance. *ND* is defined as the distance to the coast divided by the sum of the distance to the coast and the distance to the inland edge of the sedimentary basin. *ND* is meant to be a proxy for soil density/age, and it could also be considered a proxy for saturation

because the water table generally becomes shallower at shorter distances to the coast. A grid of *ND* values for Switzerland was computed using the distances from lakeshores and the boundaries of the SED geological class [7] “Alluvial plains”. The liquefaction model of [29] shows a favourable portability to the Swiss context provided high-resolution geographic datasets are used and the results are convolved with geotechnical information on ground types and water content.

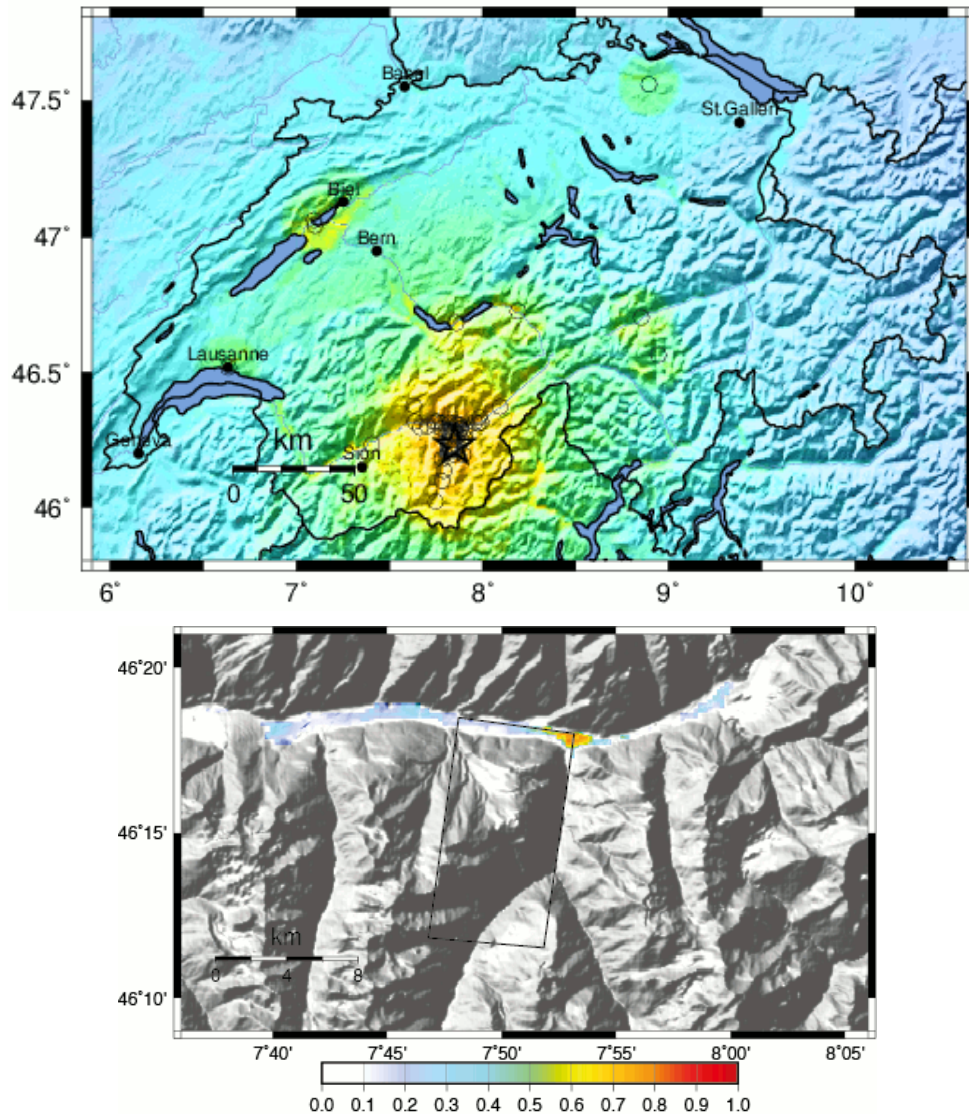


Fig. 4 – Top: ShakeMap historical scenario for the 1946 M_w 6.2 Visp-Stalden (Valais, SW Switzerland) event, including macroseismic intensity data points from ECOS-09 shown as circles. The intensity colorscale is the same as Fig. 1. Bottom: Liquefaction likelihood scenario for the same event computed as the average of the global model and Christchurch model no.3 of [29] and subsequently convolved with geotechnical information as explained in the text. The black rectangle shows the possible surface projection of the earthquake fault. Note the highest liquefaction probabilities in the town of Visp (NE corner of the fault), consistent with the historical records.

4. Implementation in ShakeMap

Prototype implementation in ShakeMap of the Swiss-adapted liquefaction and landslide likelihood models was carried out using a test virtual machine running ShakeMap3.5 and geographic layers with resolution ~ 90 m. 30-m resolution geographic layers can be also used, *e.g.*, the urban area of Basel where a detailed microzonation study is available. At larger scale the use of 30-m grids considerably delays the computation of the shaking layers. For implementation in Swiss ShakeMap, the use of high-resolution datasets is recommended only for events with magnitude larger than 5 and focusing on a region within 50 km of the earthquake epicenter. Implementation required: (a) modifying the program *grind* to include the GMT commands implementing the predictive models; and (b) adapting program mapping in order to create PostScript maps of the computed likelihoods using the same graphic style and colour scale of ShakeMap, as shown in Fig. 3 and 4.

5. Conclusions and outlook

We summarised in this paper the current status of the inclusion of earthquake-induced hazards in the Swiss implementation of USGS-style ShakeMap. We recall that these maps should not be used as predictions of the occurrence of individual mass movements or liquefaction occurrence; instead, they give an idea of the areas where these earthquake-induced hazards are most likely. While we welcome and encourage community efforts (*e.g.*, [23, 29, 42, 43, 44] and subsequent updates) to refine and update global empirical predictive models once new datasets become available (like *e.g.* for the recent earthquake sequences in Nepal in 2015, Kumamoto (Japan) and Ecuador in 2016), our preferred strategy to improve the current predictions for Switzerland focuses on collecting additional information from the Swiss Cantons (*i.e.*, the “states” of the Swiss Confederation) about mapped / known geological and geotechnical susceptibilities. One limitation of this approach is that the scale, resolution and coverage of the Cantonal maps is heterogeneous and some Cantons have mapped only instabilities that represent a potential threat to urban settlements. While this shortcoming can be partly overcome by developing statistical correlations between mapped instabilities and geological units mapped at national (federal) level, using the Cantonal data “tout court” implicitly helps us tailoring our predictions to risk prone areas of major interest to the general public, public and private stakeholders. We will also consider the inclusion in the mass-movement likelihood model of aggravation factors for known unstable slopes based on the recent works of [45, 46]. We note that the mass-movement prediction model offers a potential opportunity for rapid likelihood earthquake-triggered lake tsunami prediction, for which high-resolution bathymetry can be used as geomorphological proxy. We believe that an informative way to communicate the output of the model to the authorities and the public is to convolve the landslide likelihood information with the location of, for example, roads, railways and rivers / lakes, or postal codes, preferably within the framework of a real-time earthquake information display like [47].

6. Acknowledgements

GIS geohazard and geology were data kindly provided by: (i) Swiss Federal Office of Topography (swisstopo); (ii) Canton de Berne > Indices de dangers naturels 1:25'000 © Division des dangers naturels, Office des forêts / Cartes des dangers naturels du(des) commune(s) XY, © commune(s) XY; (iii) Canton du Valais > Centre de compétence géomatique (CC GEO) / Département des transports, de l'équipement et de l'environnement - Service des forêts et du paysage - Section dangers naturels. This work was partly supported by the Swiss National Science Foundation (SNF) program "International Short Visits", grant no. IZK0Z2_161134. We are thankful to Mike Hearne, Kate Allstadt, Eric Thompson, Bruce Worden and Vince Quitoriano for their input and suggestions.

7. References

- [1] Worden CB, Wald DJ, Allen TI, et al. (2010): A Revised Ground-Motion and Intensity Interpolation Scheme for ShakeMap. *Bull Seismol Soc Am*, **100**, 3083–3096. doi: 10.1785/0120100101
- [2] Worden, CB, Wald DJ (2016): ShakeMap Manual. <http://dx.doi.org/10.5066/F7D21VPQ>

- [3] Wald DJ, Quitoriano V, Heaton TH, et al. (1999): TriNet “ShakeMaps”: Rapid Generation of Peak Ground Motion and Intensity Maps for Earthquakes in Southern California. *Earthq Spectra* **15**, 537–555. doi: 10.1193/1.1586057
- [4] Cua G, Kästli P, Fischer M, et al. (2008): Calibrating ShakeMaps in Switzerland. *NERIES 3rd Annual Meeting*, Utrecht, Netherlands.
- [5] Edwards B, Fäh D (2013): A Stochastic Ground-Motion Model for Switzerland. *Bull Seismol Soc Am*, **103**, 78–98. doi: 10.1785/0120110331
- [6] Faenza L, Michelini A (2010): Regression analysis of MCS intensity and ground motion parameters in Italy and its application in ShakeMap. *Geophys J Int*, **180**, 1138–1152. doi: 10.1111/j.1365-246X.2009.04467.x
- [7] Fäh D et al. (2011): ECOS-09 Earthquake Catalogue of Switzerland, Release 2011 Report and Database. *Report SED/RISK/R/001/20110417*, Swiss Seismological Service ETH Zurich.
- [8] Edwards B, Michel C, Poggi V, Fäh D (2013): Determination of Site Amplification from Regional Seismicity: Application to the Swiss National Seismic Networks. *Seismol Res Lett*, **84**, 611–621. doi: 10.1785/0220120176
- [9] Hanka W, Saul J, Weber B, et al. (2010): Real-time earthquake monitoring for tsunami warning in the Indian Ocean and beyond. *Nat Hazards Earth Syst Sci*, **10**, 2611–2622. doi: 10.5194/nhess-10-2611-2010
- [10] Cauzzi C, Clinton J, Cua G, et al. (2013): The Next Generation Swiss ShakeMap: a Scientific and Technical Overview. *SSA 2013*, Salt Lake City, Utah, USA
- [11] Cauzzi C, Clinton J, Becker J, Kästli P (2013): Scwfparam: a Tool for Rapid Parameterisation of Ground Motions and Input to ShakeMap in SeisComP3. *SSA 2013*, Salt Lake City, Utah, USA.
- [12] Cauzzi C, Edwards B, Fäh D, et al. (2015): New predictive equations and site amplification estimates for the next-generation Swiss ShakeMaps. *Geophys J Int*, **200**, 421–438. doi: 10.1093/gji/ggu404
- [13] Ugai K, Yagi H, Wakai A (2013): Earthquake-Induced Landslides. doi: 10.1007/978-3-642-32238-9
- [14] Marano KD, Wald DJ, Allen TI (2009): Global earthquake casualties due to secondary effects: a quantitative analysis for improving rapid loss analyses. *Nat Hazards*, **52**, 319–328. doi: 10.1007/s11069-009-9372-5
- [15] Fritsche S, Fäh D (2009): The 1946 magnitude 6.1 earthquake in the Valais: site-effects as contributor to the damage. *Swiss J Geosci*, **102**, 423–439. doi: 10.1007/s00015-009-1340-2
- [16] Fäh D, Moore JR, Burjanek J, et al. (2012): Coupled seismogenic geohazards in Alpine regions. *Boll di Geofis Teor ed Appl*, **53**, 485–508. doi: 10.4430/bgta0048
- [17] Fritsche S, Fäh D, Schwarz-Zanetti G (2012): Historical intensity VIII earthquakes along the Rhone valley (Valais, Switzerland): primary and secondary effects. *Swiss J Geosci*, **105**, 1–18. doi: 10.1007/s00015-012-0095-3
- [18] Fine IV, Rabinovich AB, Bornhold BD, et al. (2005): The Grand Banks landslide-generated tsunami of November 18, 1929: preliminary analysis and numerical modeling. *Mar Geol*, **215**, 45–57. doi: 10.1016/j.margeo.2004.11.007
- [19] Kremer K, Hilbe M, Simpson G, et al. (2015): Reconstructing 4000 years of mass movement and tsunami history in a deep peri-Alpine lake (Lake Geneva, France-Switzerland). *Sedimentology*, **62**, 1305–1327. doi: 10.1111/sed.12190
- [20] Schwarz-Zanetti G, Deichmann N, Fäh D (2003): The earthquake in Unterwalden on September 18, 1601: A historical-critical macroseismic evaluation. *Swiss Journal of Geosciences*, **96**, 441–450.
- [21] Kaynia AM, Skurtveit E, Saygili G (2011): Real-time mapping of earthquake-induced landslides. *Bull Earthq Eng*, **9**, 955–973. doi: 10.1007/s10518-010-9234-2
- [22] Newmark NM (1965): Effects of Earthquakes on Dams and Embankments. *Géotechnique*, **15**, 139–160. doi: 10.1680/geot.1965.15.2.139
- [23] Nowicki MA, Wald DJ, Hamburger MW, et al. (2014): Development of a globally applicable model for near real-time prediction of seismically induced landslides. *Eng Geol*, **173**, 54–65. doi: 10.1016/j.enggeo.2014.02.002
- [24] Van Ballegooy S, Malan P, Lacrosse V, et al. (2014): Assessment of Liquefaction-Induced Land Damage for Residential Christchurch. *Earthq Spectra*, **30**, 31–55. doi: 10.1193/031813EQS070M
- [25] Lai CG, Bozzoni F, Mangriotis M-D, Martinelli M (2015) Soil Liquefaction during the 20 May 2012 M5.9 Emilia Earthquake, Northern Italy: Field Reconnaissance and Post-Event Assessment. *Earthq Spectra*, **31**, 2351–2373. doi: 10.1193/011313EQS002M
- [26] Roten D, Fäh D, Bonilla LF, et al. (2009): Estimation of non-linear site response in a deep Alpine valley. *Geophys J Int*, **178**, 1597–1613. doi: 10.1111/j.1365-246X.2009.04246.x
- [27] Idriss IM, Boulanger RW (2008): *Soil liquefaction during earthquakes*. Monograph MNO-12,
- [28] Ishihara K (1996): *Soil Behavior in Earthquake Geotechnics*. Oxford University Press Inc., New York, NY.
- [29] Zhu J, Daley D, Baise LG, et al. (2015): A Geospatial Liquefaction Model for Rapid Response and Loss Estimation. *Earthq Spectra*, **31**, 1813–1837. doi: 10.1193/121912EQS353M
- [30] Verdin DW, Godt J, Funk C, et al. (2007): Development of a global slope dataset for estimation of landslide occurrence resulting from earthquakes. *U.S. Geological Survey Open-File Report 2007–1188*.
- [31] Godt J, Sener B, Verdin K, et al. (2008): Rapid assessment of earthquake-induced landsliding. *Proceedings of the First World Landslide Forum*, United Nations University, Tokyo, Japan.

- [32] Nadim F, Kjekstad O, Peduzzi P, et al. (2006): Global landslide and avalanche hotspots. *Landslides*, **3**, 159–173. doi: 10.1007/s10346-006-0036-1
- [33] Selby MJ (1993): *Hillslope materials and processes*. Oxford University Press, Oxford, UK.
- [34] Jibson RW, Harp EL, Michael JA (2000): A method for producing digital probabilistic seismic landslide hazard maps. *Eng Geol*, **58**, 271–289. doi: 10.1016/S0013-7952(00)00039-9
- [35] Moore ID, Grayson RB, Ladson AR (1991): Digital terrain modelling: A review of hydrological, geomorphological, and biological applications. *Hydrol Process*, **5**, 3–30. doi: 10.1002/hyp.3360050103
- [36] Wanner E, Gruetter M (1950): Etude sur les repliques detremblement de terre du Valais, de 1946 a` 1950. *Bulletin de la Murithienne*, **LXVII**, 24–41.
- [37] Cauzzi C, Fäh D, Wiemer S, Wald J, Clinton C (2016): Towards Rapid Likelihood Estimation of Earthquake-Triggered Gravitational Mass Movements in Switzerland based on Ground-Shaking Scenarios, Geomorphology and Geotechnical Information. *SSA 2016*, Reno, Nevada, USA.
- [38] Cua G, Kästli P, Fäh D, Wiemer S, Clinton J, Giardini D (2007): Deriving Vs30 maps for Switzerland from macroseismic intensity data. *AGU2007*, San Francisco, CA.
- [39] Poggi V, Edwards B, Fäh D (2011): Derivation of a Reference Shear-Wave Velocity Model from Empirical Site Amplification. *Bull Seismol Soc Am*, **101**: 258–274. doi: 10.1785/0120100060
- [40] Marthews TR, Dadson SJ, Lehner B, et al. (2015): High-resolution global topographic index values for use in large-scale hydrological modelling. *Hydrol Earth Syst Sci*, **19**, 91–104. doi: 10.5194/hess-19-91-2015
- [41] Fäh D, Rüttener E, Noack T, Kruspan P (1997): Microzonation of the city of Basel. *J Seismol*, **1**, 87–102. doi: 10.1023/A:1009774423900
- [42] Galli P (2000): New empirical relationships between magnitude and distance for liquefaction. *Tectonophysics*, **324**, 169–187. doi: 10.1016/S0040-1951(00)00118-9
- [43] Jessee (Nowicki) MA, Hamburger MW, Wald, DJ, et al. (2016): Use of an Expanded Global Earthquake Data Set to Develop a Near Real-time Model for Predicting Seismically Induced Landslides. *SSA 2016*, Reno, Nevada, USA.
- [44] Zhu J, Baise L (2016): Updated Geospatial Liquefaction Model for Global Use. *SSA 2016*, Reno, Nevada, USA.
- [45] Kleinbrod U, Burjánek J, Fäh D (2014): Characterization of Unstable Rock Slopes Through Passive Seismic Measurements. *EGU 2014*, Vienna, Austria.
- [46] Burjanek J, Edwards B, Fäh D (2014): Empirical evidence of local seismic effects at sites with pronounced topography: a systematic approach. *Geophys J Int*, **197**, 608–619. doi: 10.1093/gji/ggu014
- [47] Cauzzi C, Behr Y, Clinton J, et al. (2016): An Open-Source Earthquake Early Warning Display. *Seismol Res Lett*, **87**, 737–742. doi: 10.1785/0220150284